

Ground state of finite nuclei evaluated from realistic interactions

Kh. Gad and H. Mütter

Institut für Theoretische Physik,

Universität Tübingen, D-72076 Tübingen, Germany

Ground state properties of finite nuclei (^{16}O and ^{40}Ca) are evaluated from realistic nucleon-nucleon interactions. The calculations are based on the Brueckner-Hartree-Fock approximation. Special attention is paid to the role of the energy spectrum for the particle states, in particular for those close to the Fermi energy. Additional binding energy is obtained from the inclusion of the hole-hole scattering term within the framework of the Green function approach. Results for the energy distribution of the single-particle strength and the sensitivity to the nucleon-nucleon interaction are investigated. For that purpose three modern nucleon-nucleon interactions are employed: the Argonne V18, the charge dependent Bonn potential and a realistic nucleon-nucleon interaction which is based on chiral perturbation theory and which has recently been fitted by the Idaho group.

I. INTRODUCTION

One of the central aims of theoretical nuclear physics is the attempt to determine the bulk properties of nuclear systems like its binding energy and its density or radius from a realistic model of the nucleon-nucleon (NN) interaction, i.e. a NN interaction which yields an accurate fit of the NN scattering data below the threshold of π -production. Quite some progress has been made during the last ten years in the determination of such realistic NN interaction models. A family of charge-dependent NN potentials has been generated, which all fit the empirical scattering data with high precision [1–3]. Nevertheless, using such NN interactions in nuclear structure calculations, one obtains results, which exhibit significant differences [4,5].

The NN interactions containing non-local terms like the charge-dependent Bonn potential [3], CDBonn, or one of the Nijmegen interaction model [1] tend to be “softer” than the purely local interactions like the Argonne V18 potential [2]. Here the expression softer interaction is used to identify those interactions which induce weaker two-nucleon correlations in the nuclear many-body wave function. This implies that the total energy of nuclear matter calculated at a given density without correlations, i.e. using the Hartree-Fock approximation, yields less repulsive results for a soft, non-local potential as compared to the energy calculated for a stiffer, local NN interaction. As an example we mention that Hartree-Fock calculations for nuclear matter at the empirical saturation density yield 4.6 MeV per nucleon using the CDBonn interaction while 30.3 MeV are obtained if the Argonne V18 potential is used [5]. Including effects of NN correlation as it is done e.g. in a Brueckner-Hartree-Fock (BHF) calculation leads to results which are attractive and much closer to each other.

All these modern interactions, however, tend to predict too much binding energy for nuclear

matter and saturation densities which are too large. This is the case for the BHF approach but is also observed if variational calculations are performed [6,7] Softer non-local interaction yield larger binding energies and saturation densities than local interactions [5]. This over-binding is often compensated by a three-nucleon force, which can be adjusted in such a way that the empirical saturation point of nuclear matter is reproduced [8–12]. These three-nucleon forces can be understood to simulate the relativistic effects as incorporated e.g. in the Dirac-BHF approach [13–16]. These three-nucleon forces, however, can also be interpreted to describe the effects of virtual excitations of nucleons to the $\Delta(3,3)$ [17,18] or N^* Roper resonance [8,19].

Phenomenological three-nucleon forces are also employed to describe the properties of light nuclei with particle number up to $A=8$ using the Green function Monte-Carlo method [20]. However, at first sight, the situation in calculating bulk properties of finite nuclei seems to be different from the corresponding situation in nuclear matter. While microscopic calculations for nuclear matter, using the modern NN interactions, yield too much binding energy, BHF calculations [21] but also calculations using the coupled cluster approach [22] predict binding energies for finite nuclei, which are too small as compared to the experimental data.

It is the aim of the present work to investigate this situation a bit more in detail. For that purpose we consider the BHF approximation paying special attention to the particle-particle excitations at low energies and including the effects of hole-hole scattering terms. We are investigating the predictions originating from various models of realistic NN interactions. These include local, like the Argonne V18 [2], and non-local models, like the CDBonn interaction [3], but also the realistic meson-exchange models based on chiral perturbation theory, which have recently been developed by the Idaho group [23].

After this introduction we will describe in section 2 a technique for the calculation of bulk properties of nuclei which account in a consistent way for short-range and long-range correlations. Results of such calculation for the nuclei ^{16}O and ^{40}Ca will be presented and discussed in section 3, which is followed by a short summary in section 4.

II. CONSISTENT TREATMENT OF LONG- AND SHORT-RANGE CORRELATIONS

The BHF approximation is one of the most popular approaches to account for effects of correlations beyond the mean-field approximation in calculating bulk properties of infinite nuclear matter and finite nuclei from realistic NN interactions. It is characterized by a solution of the Bethe-Goldstone equation, leading to the G -matrix \mathcal{G}_l ,

$$\mathcal{G}_l(\omega) = V + V \frac{Q_0}{\omega - Q_0 H_0 Q_0} \mathcal{G}_l, \quad (1)$$

and the self-consistent evaluation of the BHF single-particle energies

$$\varepsilon_i = \left\langle i \left| \frac{p^2}{2m} \right| i \right\rangle + \sum_{j < F} \langle ij | \mathcal{G}_l(\omega = \varepsilon_i + \varepsilon_j) | ij \rangle. \quad (2)$$

In these equations V stands for the bare NN interaction, Q_0 represents the Pauli operator, which restricts the propagator in the Bethe-Goldstone Eq.(1) to particle states with energies

above the Fermi energy, and i and j refer to hole-states, i.e. the eigenstates of the BHF single-particle hamiltonian with energies ε_i and ε_j below the Fermi energy. The self-consistent definition of the starting energy ω in terms of the single-particle energies is determined by the Bethe-Brandow-Petschek (BBP) theorem [24]. Since, however, the BBP theorem can only be used to justify the definition of the single-particle potential for the hole states, the optimal definition of the single-particle energies for the particle states, which enter the Bethe-Goldstone Eq.(1) because they define the eigenvalues of H_0 , has been discussed over many years in the literature. The conventional choice has been to ignore a single-particle potential or self-energy contributions for the particle states completely and approximate H_0 by the kinetic energy only. This conventional choice is supported by the coupled cluster or exponential S method [25], which using the S_2 approximation essentially leads to the same approach, This conventional choice for the single-particle spectrum of nuclear matter is not very appealing as it leads to a large gap at the Fermi surface.

Mahaux and collaborators [26] argued that it would be more natural to choose the propagator according to the Green function method, i.e. define the single-particle propagator with a single-particle energy which includes the real part of the self-energy as a single-particle potential for particle and hole states. This leads to a spectrum which is continuous at the Fermi momentum, which provided the name “continuous choice” for this approach. This continuous choice leads to an enhancement of correlation effects in the medium and tends to predict larger binding energies for nuclear matter than the conventional choice. Inclusion of three-hole-line contribution [27,28] indicate that the continuous choice seems to lead to a better convergence of the hole-line expansion and is therefore preferable. In fact, recent studies in nuclear matter show that the result is rather sensitive to details of the single-particle spectrum around the Fermi energy [29,30].

In order to investigate these effects of the low-energy particle-particle excitations, which should correspond to long-range correlations, also in finite nuclei, we follow the concept of a double partitioned Hilbert space, as it has been used before for the study of infinite nuclear matter (see e.g. [31,32]) as well as finite nuclei (see e.g. [33,34]). The long range correlations are taken into account by means of the Green function approach within a finite model space. This model space shall be defined in terms of shell-model configurations including oscillator single-particle states up certain shell. For our studies of ^{16}O and ^{40}Ca we have chosen to include configurations up to the pf shell and sdg shell, respectively. It turned out that the final results are not very sensitive to this choice. This is due to the fact that the effect of short-range correlations, i.e. originating from configurations outside this model space are not ignored but taken into account by means of an effective interaction, i.e. a G -matrix appropriate for this model space. This effective interaction \mathcal{G} is determined as the solution of the Bethe-Goldstone equation

$$\mathcal{G}(\omega) = V + V \frac{Q_{\text{mod}}}{\omega - Q_{\text{mod}} H_0 Q_{\text{mod}}} \mathcal{G}. \quad (3)$$

The Pauli operator Q_{mod} is defined to exclude two-particle states with one of the particles below the Fermi level of the nucleus considered or with both nucleons in states inside the model space. With this G -matrix we solve the BHF Eq.(2) using the self-consistent definition of the starting energy ω for hole states but also for the oscillator particle states, which are

inside the model space. We consider two different choices for the spectrum of the high-lying particle states outside the model space, defined by H_0 in Eq.(3): The conventional choice, i.e. H_0 is just the operator of the kinetic energy for the interacting particles, and the continuous choice, for which we add an attractive constant to the kinetic energy. This constant is determined in such a way, that it corresponds to the mean value of the potential energies of the low-lying particle states inside the model space.

Note that this approximate BHF scheme only accounts for particle-particle correlations outside the model space. We will call these correlations short-range correlations in the discussion below. A measure for these short-range correlations is given by the depletion coefficient

$$\kappa_i = - \sum_{j < F} \left\langle ij \left| \frac{\partial \mathcal{G}}{\partial \omega} \right| ij \right\rangle \quad (4)$$

or the corresponding occupation probability

$$\rho_i^{\text{SR}} = 1 - \kappa_i. \quad (5)$$

Using the single-particle energies we define an effective interaction for the model space in terms of the oscillator matrix elements

$$\langle ij | \mathcal{V} | kl \rangle = \frac{1}{2} [\langle ij | \mathcal{G}(\omega = \varepsilon_i + \varepsilon_j) | kl \rangle + \langle ij | \mathcal{G}(\omega = \varepsilon_k + \varepsilon_l) | kl \rangle]. \quad (6)$$

The effects of long-range correlations or correlations inside the model space shall be evaluated by means of the Green function method. To determine the correlated single-particle Green function for a nucleon with isospin τ , orbital angular momentum l and total angular momentum j one has to solve a Dyson equation, which in the case of a finite system with spherical symmetry and within a discretize model space takes the form

$$g_{\tau lj}(n, n'; \omega) = g_{\tau lj}^{(BHF)}(n, n'; \omega) + \sum_{n'', n'''} g_{\tau lj}^{(BHF)}(n, n''; \omega) \Delta \Sigma_{\tau lj}(n'', n'''; \omega) g_{\tau lj}(n''', n'; \omega), \quad (7)$$

where $g_{\tau lj}^{(BHF)}(n, n''; \omega)$ refers to the BHF propagator, which we assume to be diagonal in the radial quantum numbers n, n'

$$g_{\tau lj}^{(BHF)}(n, n'; \omega) = \delta_{n, n'} \frac{1}{\omega - \varepsilon_{n\tau lj} \pm i\eta}. \quad (8)$$

The correction to the BHF self-energy in terms of two particle one hole ($2p1h$) and two hole one particle ($2h1p$) configurations inside the model space

$$\Delta \Sigma_{\tau lj}(n, n', \omega) = \Sigma_{\tau lj}^{(2p1h)}(n, n', \omega) + \Sigma_{\tau lj}^{(2h1p)}(n, n', \omega), \quad (9)$$

is defined in terms of the effective interaction \mathcal{V} of Eq.(6). As an example we consider the $2p1h$ contribution of second order in \mathcal{V}

$$\Sigma_{\tau lj}^{(2p1h)}(n, n', \omega) = \frac{1}{2} \sum_{h < F} \sum_{p_1, p_2 > F} \frac{\langle nh | \mathcal{V} | p_1 p_2 \rangle \langle p_1 p_2 | \mathcal{V} | n'h \rangle}{\omega - (\varepsilon_{p_1} + \varepsilon_{p_2} - \varepsilon_h) + i\eta}. \quad (10)$$

In order to evaluate the total energy of the system and expectation values of one-body operators one has to rewrite the single-particle Green function in the Lehmann representation

$$g_{\tau lj}(n, n'; \omega) = \sum_{\alpha} \frac{S_{\tau lj}^p(n, n', \omega_{\alpha \tau lj})}{\omega - \omega_{\alpha \tau lj} + i\eta} + \sum_{\beta} \frac{S_{\tau lj}^h(n, n', \omega_{\beta \tau lj})}{\omega - \omega_{\beta \tau lj} - i\eta}. \quad (11)$$

The single-particle density matrix is then defined in terms of the hole-spectral function

$$\rho_{\tau lj}(n, n') = \sum_{\beta} S_{\tau lj}^h(n, n', \omega_{\beta \tau lj}) \quad (12)$$

and the total energy can be evaluated from

$$E = \sum_{\tau lj \beta n, n'} \frac{(2j+1)}{2} S_{\tau lj}^h(n, n', \omega_{\beta \tau lj}) \left\langle n \left| \frac{p^2}{2m} + \omega_{\beta \tau lj} \right| n' \right\rangle. \quad (13)$$

In order to obtain the spectral function and the positions of the poles in the single-particle Green function, $\omega_{\beta \tau lj}$, we reformulate the Dyson equation into an eigenvalue problem [21,33]

$$\begin{pmatrix} \varepsilon_1 & & 0 & a_{11} & \dots & a_{1P} & A_{11} & \dots & A_{1Q} \\ & \ddots & & \vdots & & \vdots & \vdots & & \vdots \\ 0 & & \varepsilon_N & a_{N1} & \dots & a_{NP} & A_{N1} & \dots & A_{NQ} \\ a_{11} & \dots & a_{N1} & e_1 & & & 0 & & \\ \vdots & & \vdots & & \ddots & & & & \\ a_{1P} & \dots & a_{NP} & 0 & & e_P & & & 0 \\ A_{11} & \dots & A_{N1} & & & E_1 & & & \\ \vdots & & \vdots & & & & \ddots & & \\ A_{1Q} & \dots & A_{NQ} & 0 & \dots & 0 & \dots & E_Q & \end{pmatrix} \begin{pmatrix} X_{0,1}^{\alpha} \\ \vdots \\ X_{0,N}^{\alpha} \\ X_1^{\alpha} \\ \vdots \\ X_P^{\alpha} \\ Y_1^{\alpha} \\ \vdots \\ Y_Q^{\alpha} \end{pmatrix} = \omega_{\alpha} \begin{pmatrix} X_{0,1}^{\alpha} \\ \vdots \\ X_{0,N}^{\alpha} \\ X_1^{\alpha} \\ \vdots \\ X_P^{\alpha} \\ Y_1^{\alpha} \\ \vdots \\ Y_Q^{\alpha} \end{pmatrix}, \quad (14)$$

where for simplicity we have dropped the corresponding conserved quantum numbers for isospin, parity and angular momentum (τlj). The matrix to be diagonalized contains the BHF hamiltonian defined in terms of the N BHF single-particle energies of the symmetry assumed within the model space, the coupling to the P different $2p1h$ configurations and Q $2h1p$ states. These couplings are expressed in terms of the matrix elements

$$a_{mi} = \langle mh | \mathcal{V} | p_1 p_2 \rangle \quad \text{and} \quad A_{mj} = \langle mp | \mathcal{V} | h_1 h_2 \rangle. \quad (15)$$

As long as we are still ignoring any residual interaction between the various $2p1h$ and $2h1p$ configurations the corresponding parts of the matrix in (14) are diagonal with elements in terms of single-particle energies and denoted by e_i (E_j) for $2p1h$ ($2h1p$) configurations, respectively. One can easily improve this approach and incorporate the effects of residual interactions between the $2p1h$ configurations or $2h1p$ configurations. One simply has to modify the corresponding parts of the matrix in Eq.(14) and replace where \mathcal{H}_{2p1h} and \mathcal{H}_{2h1p} contain the residual interactions in the $2p1h$ and $2h1p$ subspaces

$$\begin{pmatrix} e_1 & \dots & 0 \\ \vdots & \ddots & \\ 0 & \dots & e_P \end{pmatrix} \implies \mathcal{H}_{2p1h}, \quad \text{and} \quad \begin{pmatrix} E_1 & \dots & 0 \\ \vdots & \ddots & \\ 0 & \dots & E_Q \end{pmatrix} \implies \mathcal{H}_{2h1p}. \quad (16)$$

For the calculations which we are going to discuss here, we only consider the matrix elements for the particle-particle interaction in \mathcal{H}_{2p1h} and the hole-hole interaction for \mathcal{H}_{2h1p} . This implies that the corresponding particle-particle and hole-hole ladder diagrams are taken into account. A more complete treatment of the residual interaction requires the treatment of three-body terms and has recently been discussed e.g. by Barbieri et al. [36]

The eigenvalues ω_α of Eq.(14) correspond to the poles of the single-particle Green function in Eq.(11) and the spectral function is given in terms of the components of the eigenvectors by

$$S^h(n, n'; \omega_\alpha) = X_{0,n}^\alpha X_{0,n'}^\alpha \quad (17)$$

for eigenvalues ω_α below the Fermi energy E_F , while a corresponding equation holds for the spectral function S^p for energies above E_F .

III. RESULTS AND DISCUSSION

As a first example we would like to consider some results displayed in table I evaluated for the nucleus ^{16}O using the CDBonn potential [3] supplemented by the Coulomb interaction between protons. For the results displayed in this table the single-particle wave functions have been constrained to wave functions of the harmonic oscillator defined in terms of an harmonic oscillator constant

$$b = \frac{1}{\sqrt{2\alpha}}, \quad (18)$$

with $\alpha = 0.4 \text{ fm}^{-1}$. This corresponds to an oscillator frequency of

$$\hbar\omega = \frac{(\hbar c)^2}{mc^2 b^2} \quad (19)$$

of 13.27 MeV and leads to a radius for ^{16}O , assuming simple shell model occupancies, of 2.65 fm, which is close to the empirical value. The first two columns of table I refer to BHF calculation assuming the conventional and a continuous choice for the spectrum of the particle states in the Bethe-Goldstone equation (1). It should be recalled that we define the continuous spectrum in terms of the kinetic energy shifted by a constant such that the single-particle energies for low-lying particle states is identical to the mean value of the corresponding BHF single-particle energies calculated according to (2). Beside the single-particle energies also the occupation probabilities ρ_i^{ST} calculated according to Eq. (5) are listed. Comparing these two columns one can see that the use of a continuous single-particle spectrum leads to more attractive single-particle energies and a binding energy, which is enhanced by about 2 MeV per nucleon. This enhancement of the attraction is accompanied by lower occupation probabilities ρ_i^{ST} , which implies larger values for the corresponding depletion coefficients. This demonstrates that the lowering of the particle-state spectrum, going from the conventional to the continuous choice, leads to a substantial enhancement of correlations.

The third and fourth column of table I, labeled BHF0 and BHF(mod), refer to the model space approach as introduced in the preceding section. The BHF0 approach identifies the

BHF calculation using the G-matrix defined in (3) with a continuous choice for the particle state spectrum. This means that due to the Pauli operator Q_{mod} the contribution of low-lying particle states (for the present example those in the 1s0d and 1p0f shell) to the G-matrix are suppressed. This leads to larger occupation probabilities (compare BHF0 with BHF (cont)) and less attractive single-particle energies. Also the binding energy per nucleon is reduced by about 1 MeV.

The contribution of the low-lying particle-particle configurations are again included in the BHF(mod) approach by considering the corresponding (2p1h) component in the definition of $\Delta\Sigma$ in Eq.(9) and solving Eq.(14) ignoring the coupling to the (2h1p) configurations but allowing for the residual interaction between the particle states according to Eq.(16). In this way the effects of the low-lying particle-particle configurations are taken into account allowing for individual single-particle energies ε_{nlj} for all sub-shells with quantum numbers nlj and not just a replacement of these single-particle energies with the kinetic energy shifted by a global constant as it was done in the BHF (cont) approach discussed above. This more sophisticated treatment of the low-lying particle spectrum leads to some additional attraction in the single-particle energies ranging from 0.9 MeV in the case of the $s_{1/2}$ shell over 1.6 MeV ($p_{3/2}$) to 1.8 MeV in the case of the $p_{1/2}$ shell. The effect is obviously larger for states closer to the Fermi energy as these states are more sensitive to the details of the long-range correlations. The same feature can also be observed in the occupation probabilities ρ_{lj} . It should be pointed out that the results listed for the BHF (mod) approach accounts for depletion due to the excitation of particle state configurations inside the model space by means of Eq.(12) while the depletion due to short-range correlations leading to excitations outside the model space are accounted for by means of Eq.(5). The more specific treatment of the low-lying particle-particle configuration reduces the spin-orbit splitting for the protons in the p -shell from 3.4 MeV in the case of BHF(cont) to 3.1 MeV in the BHF(mod) approach, both values being much smaller than the experimental one (6.3 MeV).

For all approaches discussed so far, the single-particle strength for the hole states is just concentrated in one quasiparticle state. The corresponding Green functions exhibit only one pole below the Fermi energy. A distribution of this hole-strength is obtained if we also account for the 2h1p contribution in the definition of the self-energy in Eq.(9). This distribution is defined in terms of the eigenvalues ω_α in Eq.(14) and the strength defined in Eq.(17). Results for the spectral distribution are displayed in Fig. 1. In the upper panel of this figure, referring to the removal of protons with $s_{1/2}$ quantum numbers, the strength is widely distributed. In the column labeled “Green” of table I we give the mean value of this spectral distribution defined by

$$\varepsilon_{\tau lj} = \frac{\sum_{\beta n} \omega_{\beta\tau lj} S_{\tau lj}^h(n, n, \omega_{\beta\tau lj})}{\sum_n \rho_{\tau lj}(n, n)} \quad (20)$$

but also the energy of the quasiparticle state (in brackets), which is defined by that eigenvalue $\omega_{\beta\tau lj}$, which carries the largest strength. Inspecting Fig. 1 and the corresponding numbers in table I, one finds that the quasiparticle state for the $s_{1/2}$ state carries only rather little strength.

The quasiparticle contribution is much more important for the $p_{3/2}$ and $p_{1/2}$ states. For these more weakly bound states the quasiparticle states are also those which are closest to the

Fermi energy, which means that they correspond to the removal of a nucleon leading to the ground state or lowest excited state of the daughter nucleus of given parity (l) and angular momentum (j). Therefore one should consider those quasiparticle energies in comparing with experimental removal energies for these states (values presented in the last column of table I). The spin-orbit splitting resulting from these quasiparticle energies is slightly larger than the one derived from BHF(mod) approximation but still too small as compared with the experimental value. Here it should be recalled that a substantial enhancement of the spin-orbit splitting is obtained if the relativistic features of the Dirac Brueckner Hartree Fock approximation are taken into account [35].

Comparing the results of the Green function approach with those obtained in the BHF(mod) approximation, one finds that the hole-hole terms which are included in the Green function approach tend to reduce the binding energy of the quasiparticle state but lead to more attractive mean values of the spectral distribution for the hole states. Since this mean value enters the evaluation of the total binding energy (see Eq.(13)) we also get a slightly larger binding energy in the Green function approach as compared to the BHF(mod) approximation. It is worth mentioning that the Green function approach with inclusion of 2h1p terms in the self-energy also provides non-vanishing occupation probabilities for states which are unoccupied in the simple shell model. Also these occupancies contribute to the total binding energy.

At this stage it is useful to make a first comparison with the situation in corresponding calculations of nuclear matter. It has been observed also for nuclear matter that the results of BHF calculations are rather sensitive to the choice of the spectrum for the particle states, in particular for those with momenta close to the Fermi momentum [29,30]. Using the precise single-particle spectrum rather than a quadratic parametrisation leads to an increase of the binding energy in nuclear matter around saturation density of about 1.5 MeV per nucleon [30]. This is even more than the gain in binding energy from the BHF(cont) to the BHF(mod) approach displayed in table I. Also in nuclear matter one observes that the inclusion of the 2h1p terms in the self-energy lead to less attractive quasiparticle energies. The spread of the single-particle strength to lower energies, however, leads to additional binding energy. This feature, less attractive quasiparticle energies but more binding energy per nucleon, helps to fulfill the Hugenholtz - Van Hove theorem [37,38] for nuclear matter. The gain in binding energy due to the 2p1h components in the self-energy is about 0.5 MeV per nucleon in nuclear matter at saturation density [30]. Also this is a result rather similar to the difference between the BHF(mod) approach and the result of the complete Green function listed in table I.

For a first comparison of results originating from different NN interactions, we list in table II results of the Green function calculation for ^{16}O using the charge-dependent Bonn interaction [3] (CD Bonn), the version A of the Idaho interaction [23] (Idaho A), which is based on features of chiral perturbation theory, and the Argonne V18 interaction [2]. All interaction models yield quasiparticle energies which are more attractive than the experimental removal energies but a total binding energy which is slightly smaller than the empirical energy of 7.98 MeV per nucleon.

The prediction for the spectral strength of the $p_{3/2}$ and $p_{1/2}$ quasiparticle states range between 0.71 and 0.75. These values are larger than spectroscopic factors deduced from nucleon knock-out experiments, $(e, e')p$, which are around 0.6 [39]. The local NN interaction Argonne

V18 is stiffer than the non-local meson-exchange interaction models CD Bonn and Idaho A (see also the comparison in nuclear matter [30]). This means that it predicts stronger correlations, as indicated by the smaller spectroscopic factors, and smaller binding energy. Altogether one may argue that the bulk properties of ^{16}O are very well reproduced. All interactions reproduce the total energy within 1 MeV per nucleon and predict a radius for the proton distribution of 2.72 fm, which is in very good agreement with the experiment. Here, however, one must keep in mind that the radius is to a large extent determined by the choice of the oscillator parameter for the model space. The choice of $\alpha = 0.4$ has been made to obtain a radius of 2.65 fm for the uncorrelated shell-model wave function. Correlations within the model space lead to small enhancements, only. In order to test the sensitivity of the calculation on the oscillator parameter, we have performed calculations for various values of α . Results for the binding energy of ^{16}O obtained in the Green function approach are displayed in Fig. 2 as a function of the oscillator parameter α . These figures show that an energy minimum is obtained for α around 0.475 fm^{-1} (0.45 fm^{-1} , 0.44 fm^{-1}) using the CD Bonn, the Idaho A and the Argonne V18 interaction, respectively. The corresponding radii of the proton distribution are 2.29 fm, 2.41 fm and 2.48 fm, all of them too small as compared to the experimental value. Therefore the situation for calculating bulk properties of ^{16}O is similar to the attempts of evaluating the saturation point of nuclear matter. The calculation tends to predict a radius which is too small or a density which is too large. It is worth noting, however, that the disagreement for nuclear matter is larger.

As a second example we also consider the nucleus ^{40}Ca . In this case we consider a model space, which is defined in terms of harmonic oscillator wave functions including all shells up to the $2s1d0g$ shell. For a first comparison we fix the oscillator constant to $\alpha = 0.35 \text{ fm}^{-1}$. This corresponds to the simple shell model prediction for the radius of 3.5 fm, in reasonable agreement with the empirical value of 3.48 fm.

Examples for the spectral distribution are displayed in Fig. 3 (assuming the CD Bonn interaction) and numerical results obtained in the Green function approach are listed in table III. Since we have two quasiparticle states for the $s_{1/2}$ channel in the BHF approximation (see upper panel of Fig. 3), we also list two energies and occupation probabilities for this partial wave in table III. Also for this nucleus one obtains a broad distribution of the spectral strength. A well defined quasiparticle peak only shows up for the states in the $1s0d$ shell.

Also in this case, the predictions for the removal energy (absolute value of the quasiparticle energy for $d_{3/2}$), are larger than the experimental value of 8.3 MeV. Note, however, that the inclusion of $2h1p$ contributions in the Green function approach reduces the discrepancy by more than 3 MeV as compared to the BHF(mod) approximation. On the other hand, the calculated binding energies are in good agreement with the experimental value of 8.55 MeV per nucleon. So again, the calculation of bulk properties of ^{40}Ca is rather successful, if one fixes the radius with the appropriate choice of the oscillator constant α , which defines the basis of the model space.

If one releases this constraint and considers various values for α one obtains results as displayed in Figs. 4 and 5. Also in this case we observe that the minima occur for oscillator parameters which are larger than $\alpha = 0.35 \text{ fm}^{-1}$, which means that the corresponding radii are smaller than the empirical one. This is true for the various approximations (see Fig. 4) but also for the various interactions (see Fig. 5).

The comparison of the various approximation schemes in Fig. 4 confirms the conclusions,

which have been given above for the case of ^{16}O . In the case of ^{40}Ca , however, all interactions predict too much binding energy and a radius, which in the case of CD Bonn interaction is about 25 percent smaller than the experimental value. This corresponds to an average density, which is too large by about a factor of two, a situation which is approaching the situation of nuclear matter. Also in this case, the stiffer interaction Argonne V18 yields less energy and smaller densities than the softer interactions (Idaho A and CD Bonn).

IV. CONCLUSIONS

Starting from the Brueckner-Hartree-Fock (BHF) approach various approximation schemes have been investigated to derive bulk properties of finite nuclei from realistic NN interactions. It is observed that the results of BHF calculations, for finite nuclei as well as infinite nuclear matter [30], are rather sensitive to the spectrum of particle states, in particular those with energies close to the Fermi energy. Therefore a technique has been applied, to separate a detailed description of the low-energy excitations corresponding to long range correlations from the treatment of short-range correlations. While the effects of short-range correlations are taken into account by means of the G-matrix approximation of the BHF scheme, the long-range correlations are considered within the framework of the self-consistent evaluation of single-particle Green function. This approach includes the effects of particle-particle correlations but also corresponding hole-hole scattering terms.

If the basis of the model space is constrained to obtain the empirical value for the radius, one is able to reproduce the binding energy of nuclei (we consider ^{16}O and ^{40}Ca) within 0.5 MeV per nucleon, which is very satisfactory for a calculation based on realistic NN interaction. This success is due to the attraction which is obtained from the careful treatment of the low-lying particle-particle excitations but also due to the inclusion of two-hole one-particle configurations in the definition of the self-energy for the single-particle propagator. These terms yield a distribution of the single-particle strength and a shift of the quasiparticle energy. The repulsive shift of the quasiparticle energy for states close to the Fermi level improves the agreement with the experimental removal energies. The distribution of the strength, on the other hand, allows a gain in binding energy although the quasiparticle energies are less attractive. This helps to improve the fulfillment of the Hugenholtz - Van Hove theorem. The calculated spectroscopic factors for the quasiparticle states (around 0.7) are slightly above the empirical values (around 0.6) derived from $(e, e')p$ experiments.

If the constraining condition for the radius is released, the minima for the calculated energies lead to radii which are too small and densities which are too large. The calculated binding energies tend to be larger than the empirical values. This is more pronounced for the nucleus ^{40}Ca than for ^{16}O . This deficiency could be cured by considering the repulsive three nucleon forces [8–12], which are adjusted to describe the saturation point of infinite nuclear matter also for the calculation of finite nuclei.

- [1] V.G.J. Stoks, R.A.M. Klomp, C.P.F. Terheggen, and J.J. de Swart, *Phys. Rev. C* **49**, 2950 (1994) .
- [2] R.B. Wiringa, V.G.J. Stoks, and R. Schiavilla, *Phys. Rev. C* **51**, 38 (1995) .
- [3] R. Machleidt, F. Sammarruca, and Y. Song, *Phys. Rev. C* **53**, R1483 (1996) .
- [4] A. Polls, H. Mütter, R. Machleidt, and M. Hjorth-Jensen, *Phys. Lett. B* **432**, 1 (1998) .
- [5] H. Mütter and A. Polls, *Phys. Rev. C* **61**, 014304 (2000) .
- [6] A. Akmal and V.R. Pandharipande, *Phys. Rev. C* **56**, 2261 (1997) .
- [7] G.H. Bordbar and M. Modarres, *Phys. Rev. C* **57**, 714 (1998) .
- [8] P. Grange, A. Lejeune, M. Martzoff, and J.F. Mathiot, *Phys. Rev. C* **40**, 1040 (1989) .
- [9] B.S. Pudliner, V.R. Pandharipande, J. Carlson, and R.B. Wiringa, *Phys. Rev. Lett.* **74**, 4396 (1995) .
- [10] A. Akmal, V.R. Pandharipande, and D.G. Ravenhall, *Phys. Rev. C* **58**, 1804 (1998) .
- [11] A. Lejeune, U. Lombardo, and W. Zuo, *Phys. Lett. B* **477**, 45 (2000) .
- [12] W. Zuo, A. Lejeune, U. Lombardo, and J.F. Mathiot, preprint, nucl-th/0202076.
- [13] B. ter Haar and R. Malfliet, *Phys. Rep.* **149**, 207 (1987) .
- [14] R. Brockmann and R. Machleidt, *Phys. Rev. C* **42**, 1965 (1990) .
- [15] T. Gross-Boelting, C. Fuchs, and A. Faessler, *Nucl. Phys. A* **648**, 105 (1999) .
- [16] E. Schiller and H. Mütter, *Eur. Phys. J. A* **11**, 15 (2001) .
- [17] J. Fujita and H. Miyazawa, *Prog. Theor. Phys.* **17**, 360 (1957) .
- [18] M.R. Anastasio, A. Faessler, H. Mütter, K. Holinde, and R. Machleidt, *Phys. Rev. C* **18**, 2416 (1978) .
- [19] K. Shimizu, A. Polls, H. Mütter, and A. Faessler, *Nucl. Phys. A* **364**, 461 (1981) .
- [20] S.C. Pieper, V. R. Pandharipande, R.B. Wiringa, and J. Carlson, *Phys. Rev. C* **64**, 014001 (2001) .
- [21] H. Mütter and A. Polls, *Prog. Part. and Nucl. Phys.* **45**, 243 (2000) .
- [22] J.H. Heisenberg and B. Mihaila, *Phys. Rev. C* **59**, 1440 (1999) .
- [23] D.R. Entem and R. Machleidt, *Phys. Lett. B* **524**, 93 (2002) .
- [24] H.A. Bethe, B.H. Brandow, and A.G. Petschek, *Phys. Rev.* **129**, 225 (1963) .
- [25] H. Kümmel, K. H. Lührmann, and J. G. Zabolitzky, *Phys. Rep.* **36**, 1 (1978) .
- [26] J.P. Jeukenne, A. Lejeune, and C. Mahaux, *Phys. Rep.* **25**, 83 (1976) .
- [27] B.D. Day, *Phys. Rev. C* **24**, 1203 (1981) .
- [28] H.Q. Song, M. Baldo, G. Giansiracusa, and U. Lombardo, *Phys. Lett. B* **411**, 237 (1997) ;
Phys. Rev. Lett. **81**, 1584 (1998) ;
M. Baldo, G. Gianrisacusa, U. Lombardo, and H.Q. Song, *Phys. Lett. B* **473**, 1 (2000) .
- [29] M. Baldo and A. Fiasconaro, *Phys. Lett. B* **491**, 240 (2000) .
- [30] T. Frick, Kh. Gad, H. Mütter, and P. Czerski, *Phys. Rev. C* **65**, 034321 (2002) .
- [31] T.T.S. Kuo, Z.Y. Ma, and R. Vinh Mau, *Phys. Rev. C* **33**, 717 (1987) .
- [32] M.F. Jing, T.T.S. Kuo, and H. Mütter, *Phys. Rev. C* **38**, 2408 (1988) .
- [33] H. Mütter and L.D. Skouras, *Nucl. Phys. A* **555**, 541 (1993) .
- [34] K. Amir-Azimi-Nili, J.M. Udias, H. Mütter, L.D. Skouras, and A. Polls, *Nucl. Phys. A* **625**, 633 (1997) .
- [35] L. Zamick, D.C. Zheng, and H. Mütter, *Phys. Rev. C* **45**, 2763 (1992) .
- [36] C. Barbieri and W.H. Dickhoff, preprint nucl-th/0111058.
- [37] N.M. Hugenholtz and L. Van Hove *Pysica* **24**, 363 (1958) .
- [38] P. Czerski, A. De Pace, and A. Molinari, *Phys. Rev. C* **65**, 044317 (2002) .

- [39] M. Leuschner, J.R. Calarco, F.W. Hersman, E. Jans, G.J. Kramer, L. Lapikas, G. van der Steenhoven, P.K.A. de Witt Huberts, H.P. Blok, N. Kalantar-Nayestanaki, and J. Friedrich, *Phys. Rev. C* **49**, 955 (1994) .

	BHF (conv)	BHF (cont)	BHF0	BHF (mod)	Green	Exp
$\varepsilon_{s1/2}$	-38.19	-42.78	-40.74	-43.72	-44.00 (-47.01)	-40 ± 8
$\varepsilon_{p3/2}$	-18.14	-22.40	-20.40	-23.99	-24.29 (-20.68)	-18.45
$\varepsilon_{p1/2}$	-14.50	-19.02	-16.86	-20.86	-21.26 (-17.44)	-12.13
$\rho_{s1/2}$	0.928	0.854	0.904	0.871	0.867 (0.276)	
$\rho_{p3/2}$	0.926	0.855	0.898	0.829	0.823 (0.730)	
$\rho_{p1/2}$	0.916	0.857	0.900	0.818	0.802 (0.725)	
E/A	-4.61	-6.67	-5.66	-7.57	-7.78	-7.98

TABLE I. Single-particle energies (ε_i) and occupation probabilities (ρ_i) for protons in ^{16}O and the total energy per nucleon (E/A) as calculated from various approximations (see discussion in the text) are compared to experimental data. The calculations have been performed using the CD Bonn interaction and considering a model space defined in terms of oscillator functions with parameter $\alpha = 0.4$. The numbers in brackets refer to energy and occupation probability of the dominant quasiparticle contribution in the Green function approach. All energies are given in MeV.

	CD Bonn	Idaho A	Arg. V18
$\varepsilon_{s1/2}$	-44.00 (-47.01)	-44.00 (-47.43)	-42.38 (-45.63)
$\varepsilon_{p3/2}$	-24.29 (-20.68)	-24.00 (-20.64)	-23.12 (-19.77)
$\varepsilon_{p1/2}$	-21.26 (-17.44)	-20.87 (-17.28)	-20.26 (-16.62)
$\rho_{s1/2}$	0.867 (0.276)	0.873 (0.284)	0.830 (0.265)
$\rho_{p3/2}$	0.823 (0.730)	0.833 (0.747)	0.806 (0.723)
$\rho_{p1/2}$	0.802 (0.725)	0.821 (0.741)	0.794 (0.715)
E/A	-7.78	-7.65	-7.15

TABLE II. Results for single-particle energies, occupation probabilities and total energy per nucleon of ^{16}O calculated from the Green function approach using the CD Bonn, the Idaho A and the Argonne V18 interaction model. Further details see table I.

	CD Bonn	Idaho A	Arg. V18
$\varepsilon_{s1/2}$	-38.30 (-57.26) (-17.63)	-38.81 (-58.44) (-17.94)	-37.92 (-55.53) (-16.84)
$\varepsilon_{p3/2}$	-37.59 (-23.22)	-38.06 (-23.76)	-36.37 (-22.52)
$\varepsilon_{p1/2}$	-35.17 (-22.16)	-35.60 (-22.59)	-34.12 (-21.42)
$\varepsilon_{d5/2}$	-22.27 (-18.35)	-22.42 (-18.70)	-21.33 (-17.61)
$\varepsilon_{d3/2}$	-18.88 (-15.08)	-18.96 (-15.34)	-18.13 (-14.46)
$\rho_{s1/2}$	1.658 (0.160) (0.697)	1.674 (0.177) (0.715)	1.592 (0.142) (0.682)
$\rho_{p3/2}$	0.834 (0.123)	0.844 (0.141)	0.800 (0.151)
$\rho_{p1/2}$	0.826 (0.301)	0.838 (0.309)	0.794 (0.292)
$\rho_{d5/2}$	0.813 (0.691)	0.824 (0.709)	0.795 (0.679)
$\rho_{d3/2}$	0.796 (0.701)	0.808 (0.717)	0.780 (0.688)
E/A	-8.77	-8.91	-8.22

TABLE III. Results for single-particle energies, occupation probabilities and total energy per nucleon of ^{40}Ca calculated from the Green function approach using the CD Bonn, the Idaho A and the Argonne V18 interaction model. Further details see table I.

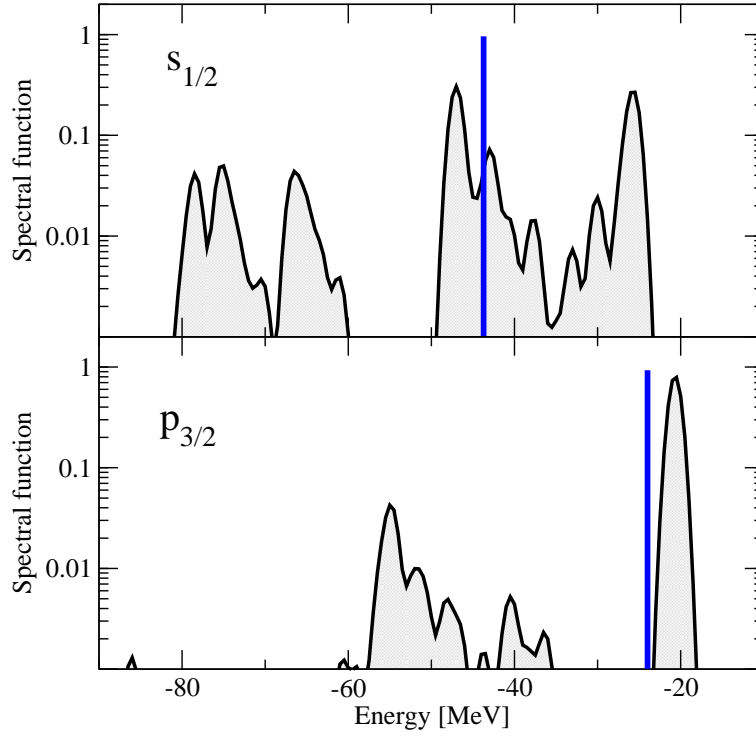


FIG. 1. The spectral function for proton hole strength in the $s_{1/2}$ (upper panel) and $p_{3/2}$ channel. The results are calculated for ^{16}O using the CD Bonn interaction. The distributions of the complete Green function approach are obtained by folding the discrete distribution with Gaussian functions assuming a width of 1 MeV. Also given are the positions of the single-particle states evaluated in the BHF(mod) approximation (straight lines).

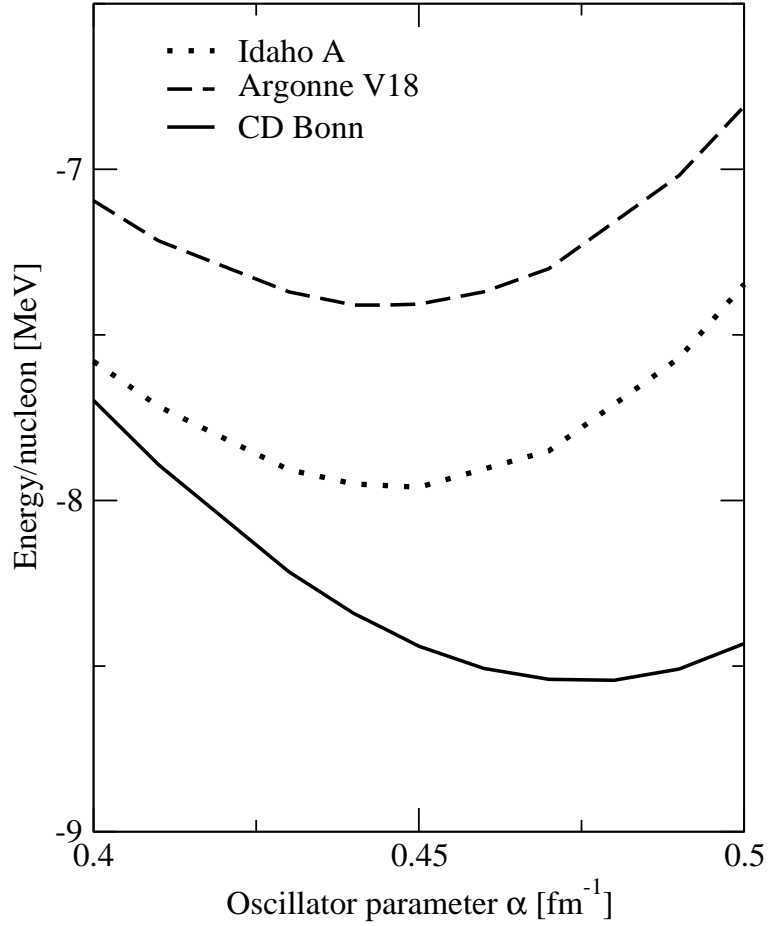


FIG. 2. Binding energy per nucleon calculated in the Green function approach as a function of the oscillator parameter α (see Eq.(18), which is used to define the basis of the model space). Results are displayed for various NN interactions

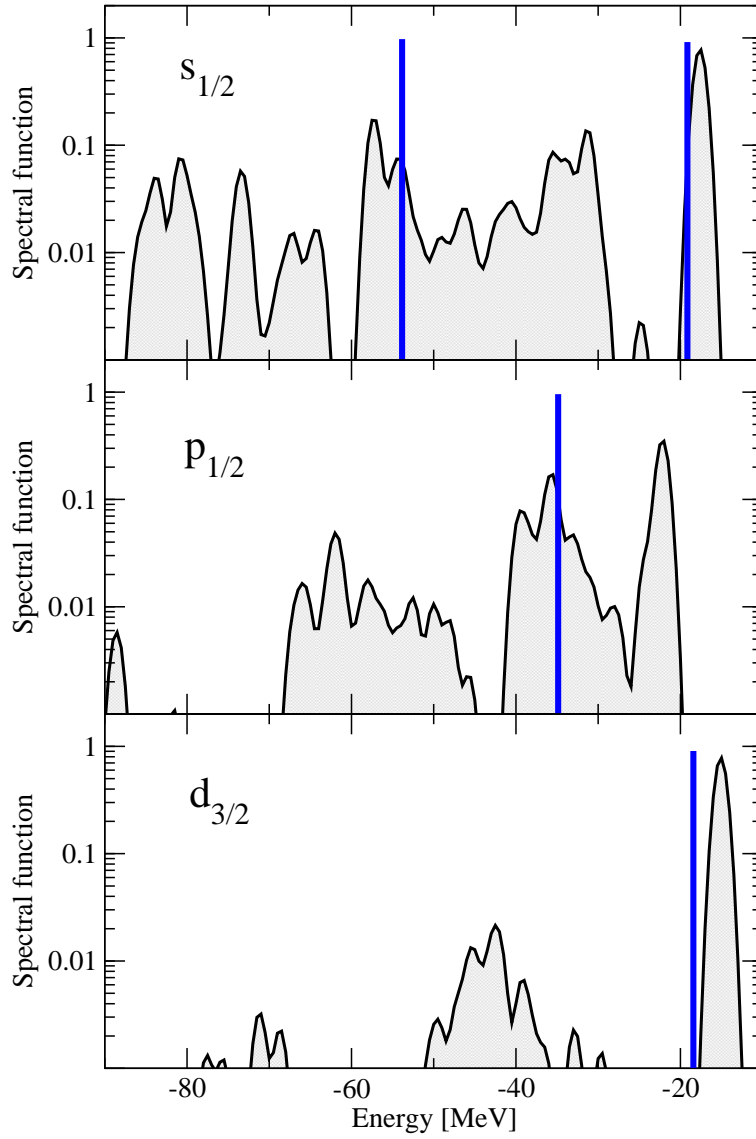


FIG. 3. The spectral function for proton hole strength in the $s_{1/2}$ (upper panel) and $p_{1/2}$ (middle) and $d_{3/2}$ channel. The results are calculated for ^{40}Ca using the CD Bonn interaction. Further details see Fig. 1.

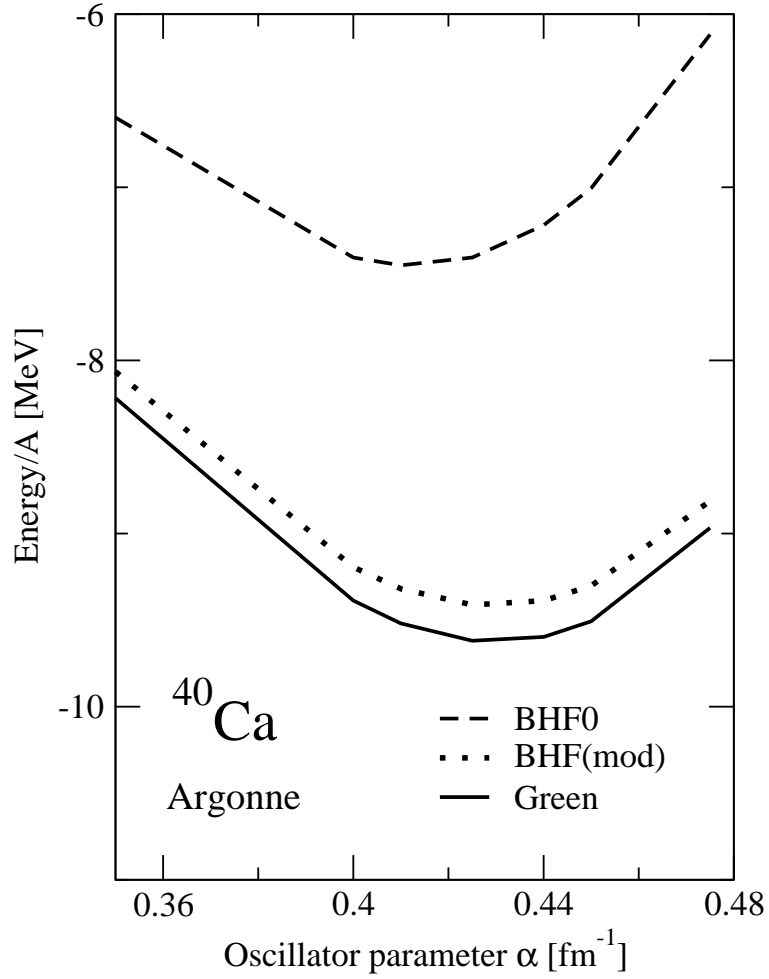


FIG. 4. Binding energy per nucleon for ^{40}Ca calculated in the Green function approach as a function of the oscillator parameter α . Results are displayed for various approximation schemes (for nomenclature see table I)

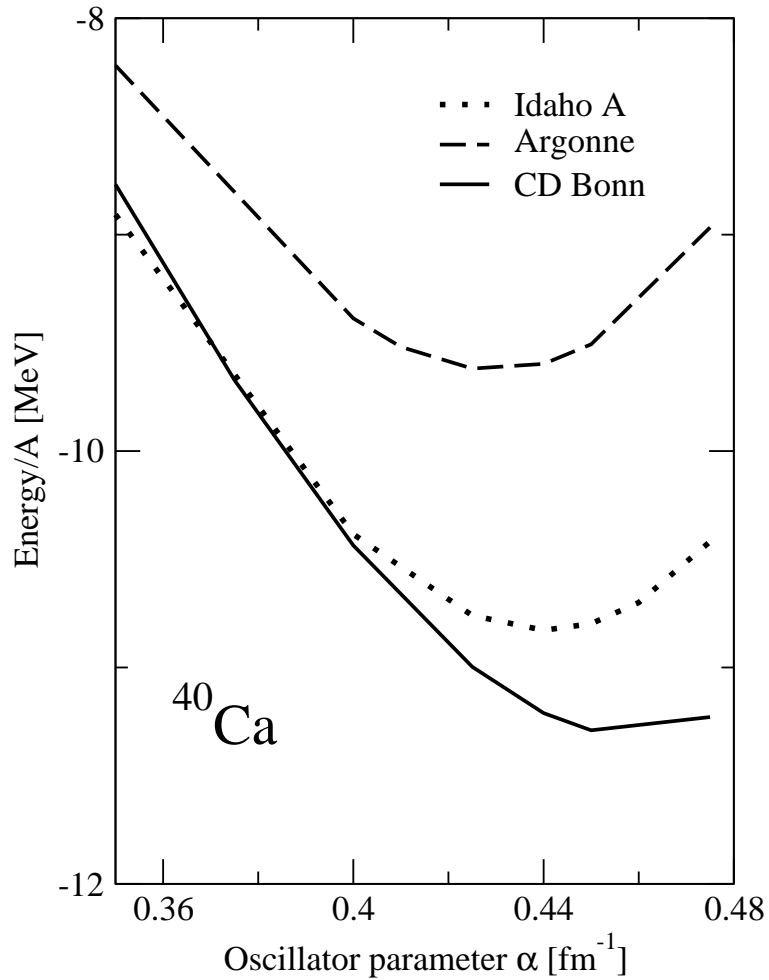


FIG. 5. Binding energy per nucleon calculated in the Green function approach as a function of the oscillator parameter α . Results are displayed for various NN interactions